LAND USE AND LAND COVER CHANGE INVESTIGATION OVER A DECADE (2000-2014) USING EARTH OBSERVATION DATASETS

6.1 INTRODUCTION

LULCC are referred as the alteration of earth's terrestrial surface due to diversified anthropogenic activities. Investigation of LULCC is essential to recognize the environmental transform processes from global to local level (Dickinson, 1995; Srivastava et al., 2012). It was also observed that LULCC are linked to most significant variable for changes affecting global ecological systems and better understanding of urban/agricultural environment development (Vitousek 1994; Lambin et al., 2003; Srivastava et al., 2012). An improved understanding of LULC changing patterns and interactions between anthropogenic activities and natural occurrences are essential for sustainable management of natural resources and decision making (Thakur et al., 2012; Rawat and Kumar, 2015). Therefore, in last few decades, it has gained ample interests in the fields of environment, ecology, habitat, biodiversity, geography, hydrology and so forth.

Nowadays, it is well known that the satellite remote sensing is an attractive pathway of acquiring accurate and timely geospatial information of the earth's surface that are very much useful in describing LULCC at local, regional and global scales (Foody, 2003; Yuan et al., 2005). Remote sensing images from various satellite sensors offer the ability to derive cost effective, rapid and accurate LULC information at different observational scales for understanding the spatio-temporal distribution of changes (Bagan et al., 2005; Bartholome and Belward, 2005; Gong et al., 2013; Zhu and Woodcock, 2014). The availability of multtemporal remote sensing images provided by Landsat series satellites at no cost supply a wealth of information for identifying and detecting LULCC and reported in several studies (Yuan et al., 2005; Otukei and Blaschke, 2010; Rawat and Kumar, 2015; Mishra and Rai, 2016). In general, LULCC detection methods are divided into pre-classification and post-classification techniques (Yuan et al., 1998). The pre-classification techniques employ various algorithms directly to multi-temporal satellite images to generate “change” and “no-change” maps. These techniques provide only location not the nature of changes (Ridd and Liu, 1998; Yuan et al., 1998). On the other hand, post-classification technique compares two or more separately classified images of different times (Mouat et al., 1993). It is considered to be the most suitable and commonly used method for change detection (Jensen, 2005). Although, the accuracy of change assessment using classified maps is strongly influenced by the individual classification accuracy. Therefore, it is key subject to effectively derive reliable LULC information from remote sensing images with reasonable accuracy using an appropriate classification technique (Yuan et al., 2005; Otukei and Blaschke, 2010).

Generally, remote sensing image classification is used to attain spatially distributed LULC information (Borak and Strahler, 1999). An appropriate classification technique is also required to derive reliable and spatially distributed LULC information effectively from remote sensing images. Several classification techniques have been reported in last few decades (Lu and Weng, 2007). The classification techniques can be broadly categorized as parametric and non-parametric classifiers. The main established parametric approach is the MLC (Maximum Likelihood classifier), which supposes a normal Gaussian distribution of data for individual classes (Jensen, 2005). It generates decision surfaces on the basis of mean and covariance of every class (Richards and Jia, 2006; Srivastava et al., 2012). In MLC, it is required to examine carefully that each class follows normal Gaussian distribution. In last two decades non-parametric approaches such as ANN and SVM have been used broadly for image classification (Kavzoglu and Mather, 2003; Singh et al., 2014; Kumar et al., 2015; Mishra and Rai, 2016). A number of ANN is developed and well established as a valuable tool for the analysis and classification of remotely sensed images (Hilbert and Ostendorf 2001; Dixon and Candade, 2008; Kavzoglu 2009; Mishra and Rai, 2016). It is popular because of advantages over statistical classification methods. However, some studies have reported difficulties in using back propagation ANN for classification of crops and other LULC categories (Foody and Arora, 1997; Kavzoglu and Mather, 2003). The SVM is based on machine learning theory proposed by Vapnik and Chervonenkis (1971). It does not make any assumption about the statistical nature of data and provides some system-inherent advantages in comparison to other classification techniques (Vapnik, 2000). It is sensitive to the size of training samples and dimensionality of the data sets (Pal and Foody, 2010). The performance of SVM have been compared with other classification techniques (Dixon and Candade, 2008; Kumar et al., 2015; Kumar et al., 2017). The high potential of SVM has attracted a great attention for image classification in remote sensing community. Several studies have also been endeavored from India, illustrating the effectiveness of remote sensing images for analyzing the nature and dynamics of LULCC (Raju and Kumar 2006; Singh et al., 2014; Misra et al., 2015; Rawat and Kumar, 2015; Mishra and Rai, 2016).

In the present study, three different classification techniques were explored for LULC classification at different years to assess the LULCC particularly in the built up and agricultural land categories. To this end, the main objectives are: (1) to evaluate and compare the classification techniques including two machine-learning algorithms (ANN, SVM) and a traditional statistical classifier (MLC), (2) to choose the best technique on the basis of LULC classification accuracy results using Landsat images and then is used to assess LULCC within the study area over the given period; (3) to perform a sophisticated statistical t-test to estimate the significance of LULCC between the study periods. The study presented here is primarily focused on the detection and analysis of spatio-temporal LULCC in Varanasi district, UP, India.

6.2 STUDY AREA

The study area for present work is Varanasi district, extending between 25°10′30″ N to 25°35′15″ N latitude and 82°40′50″ E to 83°12′18″ E longitude lies in the eastern part of Uttar Pradesh, India covering an area of around 1532.91 km^2. The location of Varanasi district as viewed on Landsat 8-OLI image is shown in the Figure 1.6 in the introduction section.

6.3 MATERIALS AND METHODOLOGY

In this study, level-one standard terrain-corrected product (L1T) of Landsat series satellites were used for LULC classification and change analysis in Varanasi district, UP, India. The multi-temporal Landsat images acquired from TM, ETM+, OLI/TIRS sensors for the period of 2000-2014 were downloaded from the USGS Earth Explorer (http://earthexplorer.usgs.gov/). Out of total downloaded images, only best suitable images of four distinct years 2000, 2005, 2009 and 2014 were chosen for LULC classification and change analysis purposes. The detailed description of images used in the present study is listed in Table 1.2.

6.3.1 Image preprocessing and data preparation

The multi-temporal Landsat images were first imported into ENVI platform and the layer stacking option available in basic tools was used to generate FCC for all the images. All the Landsat images were atmospherically corrected using QUAC module. It is obligatory to perform geometric rectification to derive spatially corrected LULC maps. So, the image-to-image registration process was applied to co-register all the datasets. During the process of image transformation, the first-degree polynomial equation and nearest neighbor resampling method was used. The images are spatially referenced in the UTM projection system (Zone 44, North) with datum WGS-1984 and the pixel size is 30 meter. Spatial subsetting was done to extract the data covering the study area. The bands used for this study includes B1–B5 and B7 for Landsat 5-TM, B1–B5, B7 and B8 for Landsat 7-ETM+ and B2–B8 for Landsat 8-OLI for the purpose of LULC classification. Using an appropriate band combination, the FCCs for all the images were generated that can be used to create training samples for classification and analysis purposes.

After this, training samples were selected and region of interest (ROI) files were generated. The training and testing samples containing various LULC classes were collected from different locations in the study area. A random sampling method was used to collect training and testing samples. One of the ROI files was used as training samples while other ROI file was used as testing samples. In total, 2034 pixels were used as the training samples, whereas 678 pixels were used as the testing samples for all the classification algorithms used in this study.

6.3.2 Spectral separability analysis

For the needs of this study, ENVI software has been used to perform separability tests on training sample using multi-temporal Landsat images listed in Table 1.2. More specifically, the Jeffries-Matusita (J-M) distance method (Richards and Jia, 2006) has been employed in this study to evaluate the spectral separability among LULC classes. It is a statistical measure of the distance between two class signatures (training samples). It facilitates to signify how well a selected spectral class pair is statistically separable. It is used mostly to appraise the quality of training samples prior to image classification to classify the classes of interest correctly to improve the accuracy of classification. Its values range between 0.0 and 2.0 and show how well the selected training samples are statistically separable (Swain and Davis, 1978). The J-M distance for two classes '*a*' and '*b*' is given as:

$$\mathrm{JM}_{\mathrm{ab}} = \sqrt{2(1 - \exp(-\alpha)} \tag{6.1}$$

$$\alpha = \frac{1}{8}(\mu_a - \mu_b)^T \left(\frac{C_a + C_b}{2}\right)^{-1} (\mu_a - \mu_b) + \frac{1}{2}\ln\left[\frac{\frac{1}{2}|C_a + C_b|}{\sqrt{|C_a||C_b|}}\right] \tag{6.2}$$

where μ_a and μ_b are mean values for classes a and b, C_a and C_b are the covariance matrices for classes a and b, and T indicates the transpose of a vector. Its values >1.7 shows that the classes are well separable while values < 1.0 shows poor separability between class pairs (ENVI User's Guide 2009). The spectral separability analysis for all class pairs was performed using multi-temporal Landsat images. The J-M method based spectral separability analysis showed better separation between almost all class pairs. Out of seven major identified LULC classes water bodies, sand and built up provided highest separability amongst all other class-pairs due to their unique spectral reflectance patterns for all the images. However, class pair of agricultural land and sparse vegetation showed comparatively lower separability due to their spectrally similar response. It may result the misclassification of agricultural land into sparse vegetation and vice-versa. In this study, the separability analysis presents the results for Landsat 7- ETM+ image of 03 April, 2000 with the range of values from 1.75 to 2.00, Landsat 5-TM image of 11 May, 2005 with the range of values from 1.75 to 2.00, Landsat 5-TM image of 23 June, 2009 with the range of values from 1.76 to 2.00, Landsat 8-OLI image of 05 June, 2014 with the range of values from 1.77 to 2.00. The results of spectral separability analysis achieved for each class pairs of respective image scenes of the study area are presented in Table 6.1.

Table 6.1 Spectral separability analysis between LULC classes using J–M distance method

	2000-Landsat 7-ETM+							2005-Landsat 5-TM						
	AL	DV	SV	FL	BU	WB	SA	AL	DV	SV	FL	BU	WB	SA
AL		1.98	1.75	1.99	1.99	2.00	2.00		1.96	1.75	1.97	1.99	2.00	2.00
DV	1.98		1.93	2.00	2.00	2.00	2.00	1.96		1.92	2.00	2.00	2.00	2.00
SV	1.75	1.93		1.99	2.00	2.00	2.00	1.75	1.92		1.99	2.00	2.00	2.00
FL	1.99	2.00	1.99		1.99	2.00	1.99	1.97	2.00	1.99		1.99	2.00	2.00
BU	1.99	2.00	2.00	1.99		2.00	2.00	1.99	2.00	2.00	1.99		2.00	2.00
WB	2.00	2.00	2.00	2.00	2.00		2.00	2.00	2.00	2.00	2.00	2.00		2.00
SA	2.00	2.00	2.00	1.99	2.00	2.00		2.00	2.00	2.00	2.00	2.00	2.00	2.00

	2009-Landsat 5-TM							2014-Landsat 8-OLI/TIRS						
	AL	DV	SV	FL	BU	WB	SA	AL	DV	SV	FL	BU	WB	SA
AL		1.99	1.76	1.98	1.99	2.00	2.00		1.98	1.77	1.99	1.99	2.0	2.00
DV	1.99		1.93	2.00	2.00	2.00	2.00	1.98		1.93	2.00	2.00	2.00	2.00
SV	1.76	1.93		1.99	2.00	2.00	2.00	1.77	1.93		1.99	2.00	2.00	2.00
FL	1.98	2.00	1.99		1.99	2.00	2.00	1.99	2.00	1.99		1.99	2.00	2.00
BU	1.99	2.00	2.00	1.99		2.00	2.00	1.99	2.00	2.00	1.99		2.00	2.00
WB	2.00	2.00	2.00	2.00	2.00		2.00	2.00	2.00	2.00	2.00	2.00		2.00
SA	2.00	2.00	2.00	2.00	2.00	2.00		2.00	2.00	2.00	2.00	2.00	2.00	

Note: AL- Agricultural land, DV- Dense vegetation, SV- Sparse vegetation, FL- Fallow land, BU- Built up, WB- Water bodies, SA- sand

6.3.3 LULC classification procedure

To investigate the changes on earth's surface and attain an accurate classification based on remote sensing image, it is of significant importance to determine the number of discrete LULC classes that are considered to be the most suitable for representation of the landscape of study area. A visual examination with good field knowledge of the study area assisted to choose the representative classes depicted at the remote sensing images. Moreover, the heterogeneity of the area of interest and the 30 m spatial resolution of Landsat images induced to come up with seven well discriminated LULC classes such as agricultural land, dense vegetation, sparse vegetation, built up, fallow land, water bodies and sand. The pre-processed multi-temporal Landsat series images are classified using supervised classification techniques such as MLC, ANN and SVM in ENVI (v 5.1) software in to identify diverse land surface features. The LULC maps for years 2000, 2005, 2009 and 2014 were derived by classifying the Landsat images of respective years. A brief description of the classification algorithms used in this study was provided in the previous chapters.

For the present study, ANN have the input layers indicating the used spectral bands of Landsat images, one hidden layer and seven neurons in the output layer as seven LULC classes. For processing of data by ANN model, the learning rate and momentum value were taken as 0.10 and 0.90 respectively. Other parameters like RMSE and numbers of training iterations are taken as 0.1 and 1000 respectively for LULC classification. The basic structure of a three layer ANN used in this study for Landsat 8-OLI image only is shown in Figure 6.1. In the same way ANN can also be structured for other datasets.

In this study, RBF kernel was used in SVM based classification. For RBF kernel, two parameters namely penalty parameter (C) and gamma parameter (γ) were set to a default values 100 and 0.14 respectively. The value of pyramid parameter was set to be zero to process the image at full resolution.

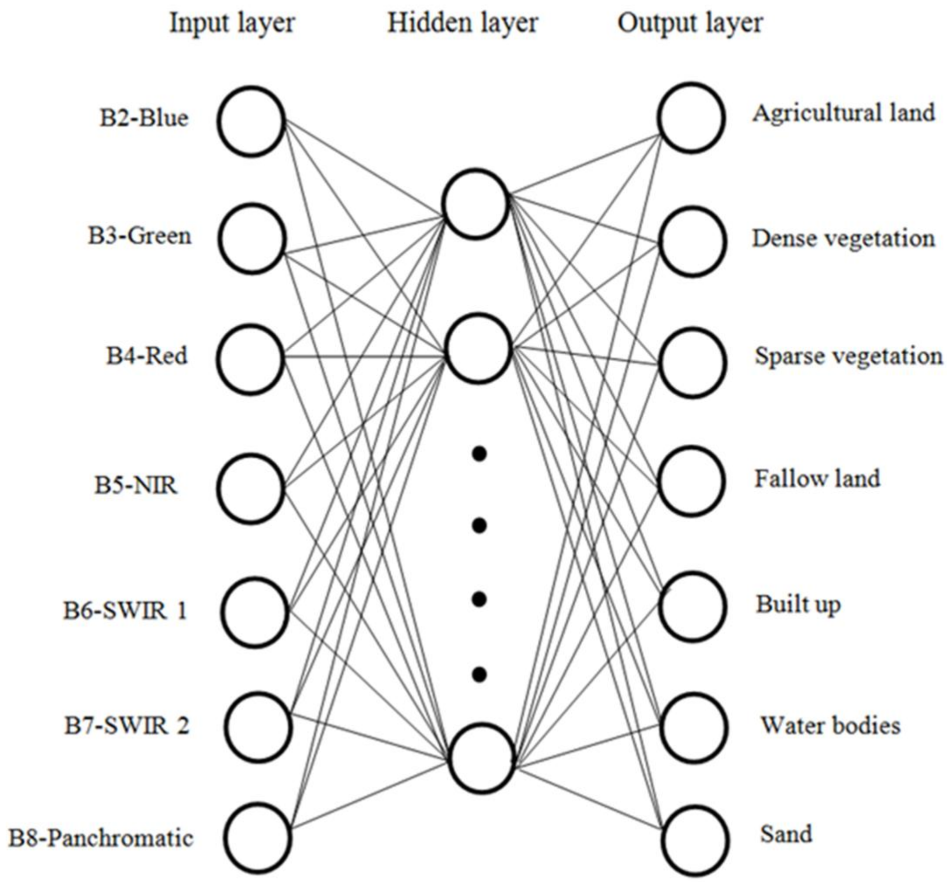

Figure 6.1 The structure of a three- layer ANN

6.3.4 Assessment of LULC classification accuracy

The confusion matrix approach was used to evaluate the accuracy of LULC classification results obtained from all the classifiers. The accuracy assessment was carried out by computing the UA, PA, OA and Kc using Equations (1.1) to (1.4). Furthermore, the F-score was computed using Equation (1.5) for better evaluation of classification accuracies of individual LULC class.

6.3.5 LULCC detection and analysis

The change analysis illustrates and quantifies the distinctions between images of the same area at different times. The classified LULC images of four different dates can be used to compute the area of different LULC classes and monitor the changes observed in the given time period. This type of quantitative analysis is very much useful to identify diverse changes occurring in different LULC classes like increase in built-up area or decrease in agricultural land and so on. In the present study, LULCC detection and analysis was based on LULC maps obtained by classifying Landsat series satellite images of years 2000, 2005, 2009 and 2014. A post-classification approach was employed to assess the changes in the area of LULC classes during a particular time period. In this study, the quantification of LULCC was carried out during 2000-2005 (period 1), 2005-2009 (period 2), 2009-2014 (period 3) and 2000-2014 (period 4) respectively. The annual rate of change (rt) for each LULC class was calculated by Equation (6.3) (Puyravaud 2003)

$$\mathrm{rt} = \frac{1}{(\mathrm{t}_2 - \mathrm{t}_1)} \times \ln\left(\frac{\mathrm{A}_2}{\mathrm{A}_1}\right) \times 100 \qquad (6.3)$$

where A_1 and A_2 are the areas (in km^2) of a LULC class at years t_1 (initial time) and t_2 (later time) respectively. A positive rt value signifies that the area of a particular LULC type is increasing, while negative indicates decreasing trend.

6.3.6 Analyses for statistical significance of LULCC

An appropriate statistical test is required to carry out a test for relationship between LULC states between all study periods. A paired samples t-test is performed to test whether the LULC changes are statistically significant or not between selected study periods. This test is parametric in nature and found to be statistically suitable for determining the difference between two time periods. A paired samples *t*-test is used to compare two population means. If there are two samples in which observations in one sample can be paired with observations in the other sample. The hypotheses can be expressed as:

$$H_0: \mu_1 = \mu_2 \text{(the paired population mean are equal)}$$

$$H_1: \mu_1 \# \mu_2 \text{(the paired population mean are not equal)}$$

The statistic for the paired samples *t*-test, indicated by t is given by formula same as the one sample *t*-test:

$$t = \frac{\bar{x}_{diff} - 0}{S_{\bar{x}}} \tag{6.4}$$

where

$$S_{\bar{x}} = \frac{S_{diff}}{\sqrt{n}} \tag{6.5}$$

where $\bar{x}_{diff}$ = Sample mean of the differences, S_{diff} = Sample standard deviation of the differences, $S_{\bar{x}}$ = Estimated standard error of the mean ($S/\sqrt{n}$), and n = sample size (ie. number of observations).

The calculated *t* value is compared to the critical *t* value with the degrees of freedom (df) = $n - 1$ for a chosen confidence level. If the calculated *t* value is greater than the critical *t* value, the null hypothesis will be rejected.

6.4 RESULTS AND DISCUSSION

6.4.1 LULC classification results using multi-temporal images

Twelve LULC classified maps were obtained corresponding to the classification of the Landsat series images of years 2000, 2005, 2009 and 2014 respectively based on different classification algorithms such as MLC, ANN and SVM. These classified LULC maps are shown in Figures 6.2, 6.3 and 6.4 respectively.

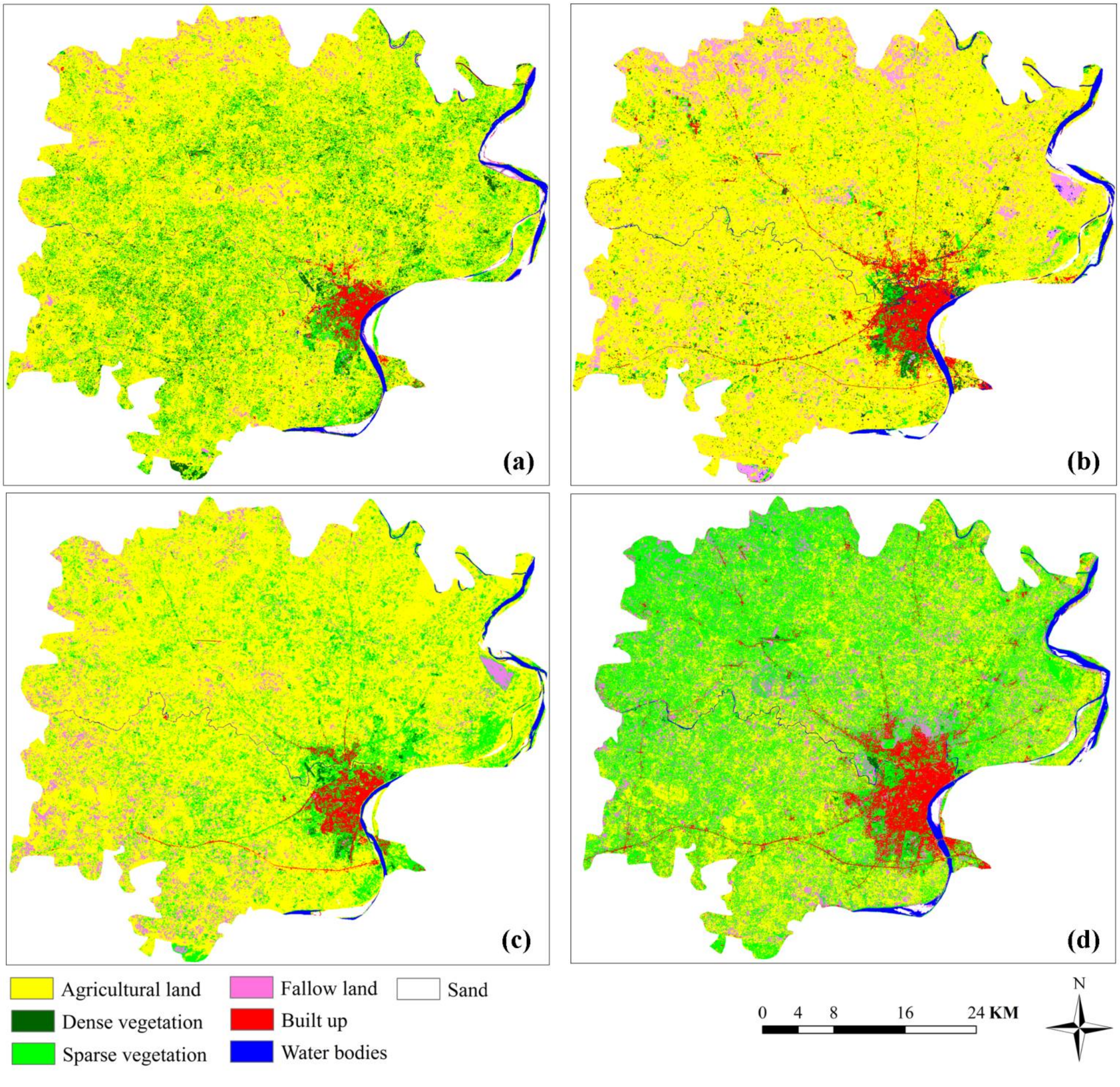

Figure 6.2 MLC based LULC classification for years (a) 2000, (b) 2005, (c) 2009, and (d) 2014

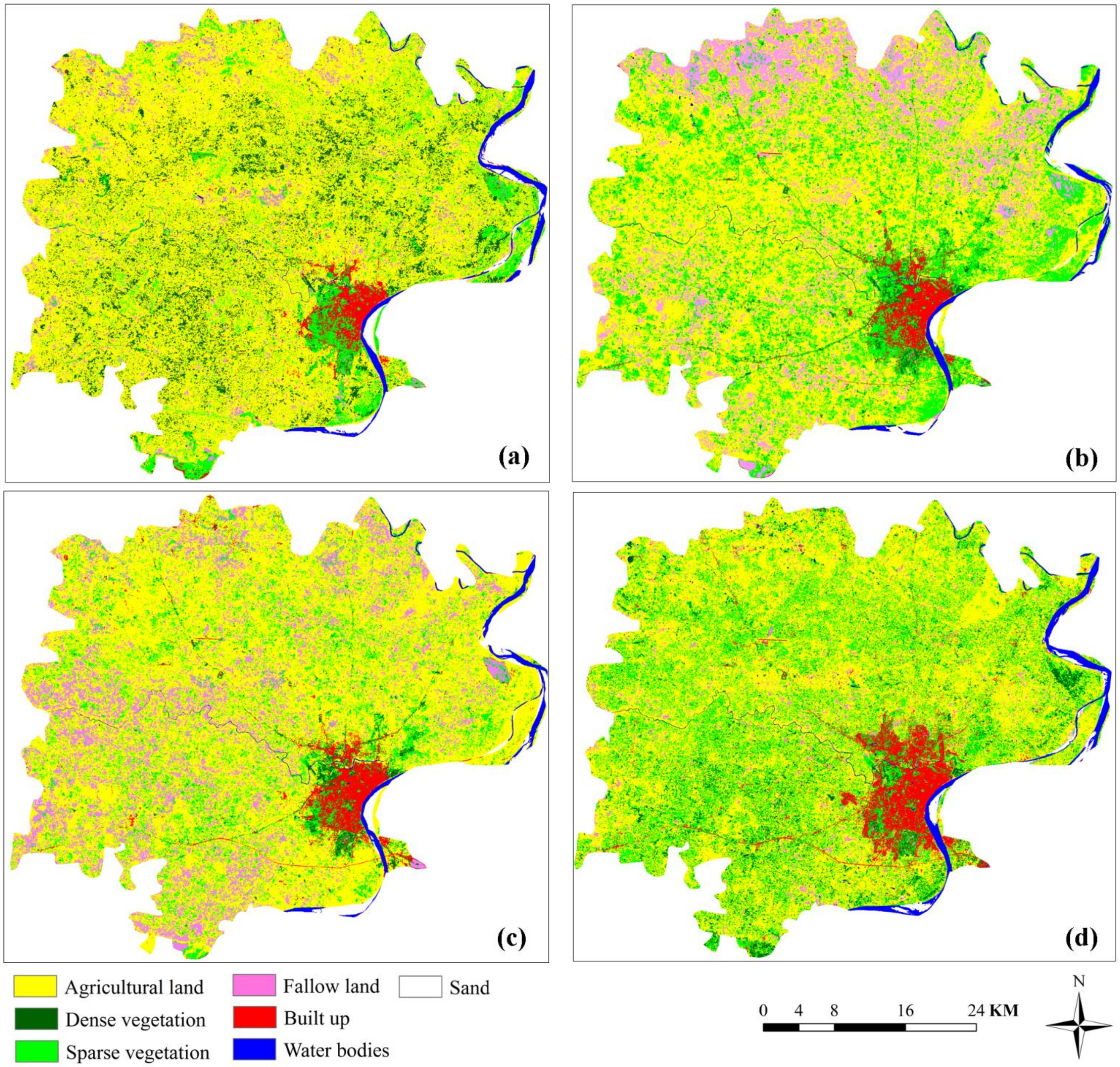

Figure 6.3 ANN based LULC classification for years (a) 2000, (b) 2005, (c) 2009, and (d) 2014

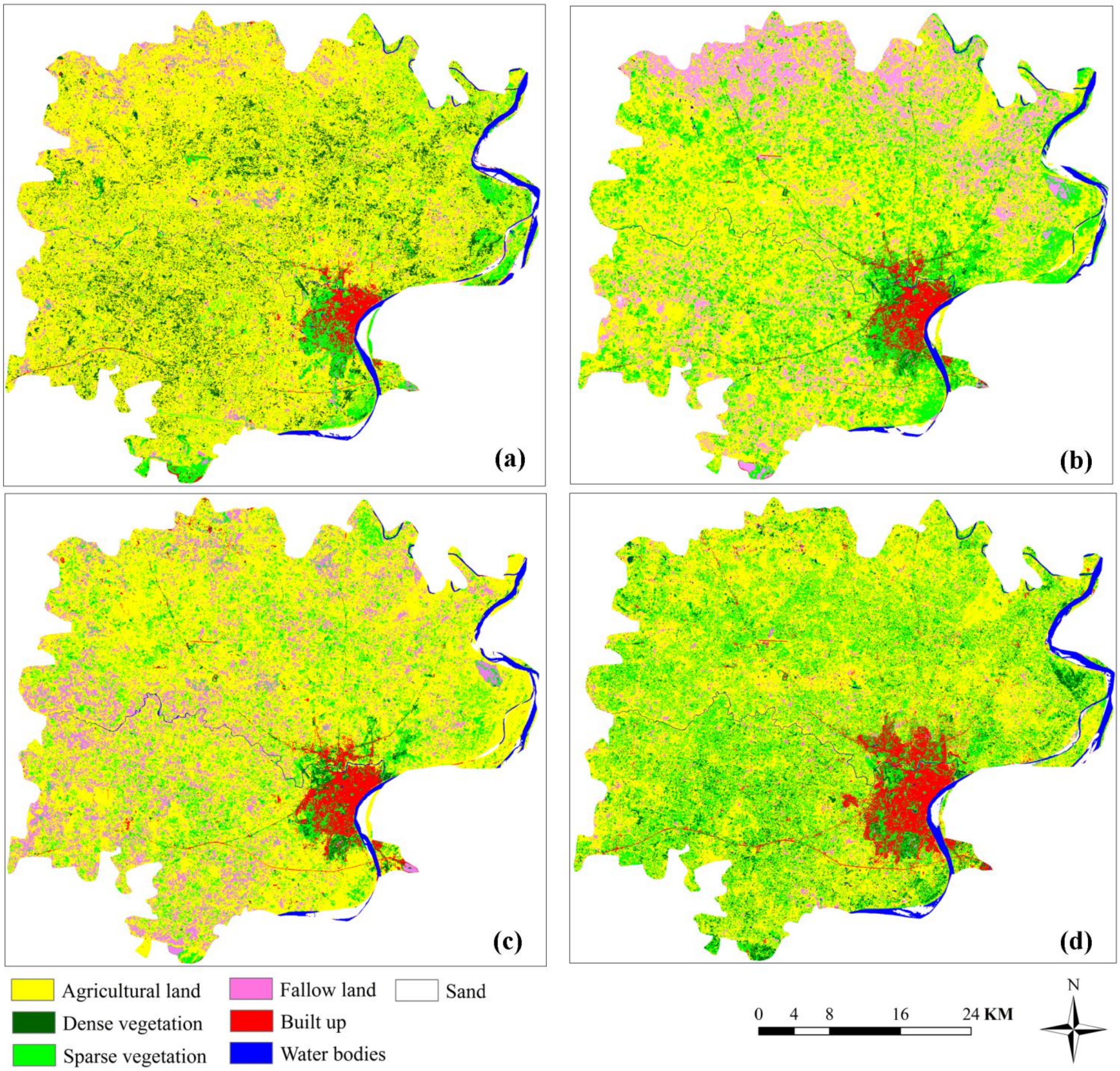

Figure 6.4 SVM based LULC classification for years (a) 2000, (b) 2005, (c) 2009, and (d) 2014

6.4.2 Accuracy assessment of LULC classification results

The evaluation of LULC classification accuracy was carried out using the confusion matrix approach for years 2000, 2005, 2009 and 2014 using three different classification methods. Each of the LULC map was compared to the ground reference data to evaluate the accuracy of the classification results. The ground reference data was collected by taking into account the random sample points, the field knowledge and Google earth.

The statistics of PA, UA, OA, Kc and F-score achieved for different years using different classification algorithms (MLC, ANN and SVM) are listed in Tables 6.2, 6.3 and 6.4.

The MLC algorithm based OA for the classified images of 2000, 2005, 2009 and 2014 were found to be 81.56%, 79.65%, 81.68% and 82.60% respectively. The Kc for the classified images of 2000, 2005, 2009 and 2014 were 0.7847, 0.7623, 0.7848 and 0.7967 respectively.

The ANN algorithm based OA for the classified images of 2000, 2005, 2009 and 2014 were found to be 84.66%, 84.07%, 85.25% and 85.84% respectively. The Kc for the classified images of 2000, 2005, 2009 and 2014 were 0.8209, 0.8140, 0.8278 and 0.8347 respectively.

The SVM algorithm based OA for the classified images of 2000, 2005, 2009 and 2014 were found to be 86.58%, 87.48%, 88.79% and 89.43% respectively. The Kc for the classified images of 2000, 2005, 2009 and 2014 are 0.8433, 0.8553, 0.8691 and 0.8760 respectively. The OA and Kc of SVM based classified image are found to be highest for all the years, followed by ANN and MLC.

Table 6.2 Accuracy assessment of LULC classification results using MLC

Year	2000			2005			2009			2014		
LULC classes	PA (%)	UA (%)	F-score (%)	PA (%)	UA (%)	F-score (%)	PA (%)	UA (%)	F-score (%)	PA (%)	UA (%)	F-score (%)
Agricultural Land	80.39	79.61	80.00	74.51	76.00	75.25	82.35	80.77	81.55	82.35	80.77	81.55
Dense vegetation	84.27	80.65	82.42	82.02	80.22	81.11	84.27	80.65	82.42	80.90	83.72	82.29
Sparse vegetation	77.36	74.55	75.93	73.58	76.47	75.00	76.64	78.10	77.36	80.19	80.19	80.19
Fallow land	84.21	86.02	85.11	81.05	79.38	80.21	85.26	83.51	84.38	84.21	82.47	83.33
Built up	80.37	83.50	81.90	83.18	80.91	82.03	80.37	83.50	81.90	83.18	81.65	82.41
Water bodies	83.37	91.76	87.64	82.80	89.53	86.03	82.80	89.53	86.03	89.25	91.21	90.22
Sand	81.40	79.10	79.10	81.40	76.09	78.65	80.95	76.40	78.61	77.91	78.82	78.36
OA (%)	81.56			79.65			81.68			82.60		
Kc	0.7847			0.7623			0.7848			0.7967		

Table 6.3 Accuracy assessment of LULC classification results using ANN

Year	2000			2005			2009			2014		
LULC class	PA (%)	UA (%)	F-score (%)	PA (%)	UA (%)	F-score (%)	PA (%)	UA (%)	F-score (%)	PA (%)	UA (%)	F-score (%)
Agricultural Land	81.37	82.18	81.77	78.43	85.11	81.63	83.33	82.52	82.93	85.29	82.86	84.06
Dense vegetation	85.39	88.37	86.86	84.27	89.29	86.71	87.64	88.64	88.14	89.89	89.89	89.89
Sparse vegetation	80.19	80.95	80.57	81.13	80.37	80.75	82.08	83.65	82.86	81.13	85.15	83.09

Fallow land	83.16	84.04	83.60	84.21	80.81	82.47	84.21	84.21	84.21	85.26	82.65	83.94
Built up	85.98	88.46	87.20	84.11	85.71	84.91	88.79	87.96	88.37	87.85	89.52	88.68
Water bodies	88.17	97.62	92.66	90.32	96.55	93.33	84.95	96.34	90.29	84.95	97.53	90.80
Sand	89.53	74.04	81.05	87.21	73.53	79.79	86.05	75.51	80.43	87.21	75.76	81.08
OA (%)	84.66			84.07			85.25			85.84		
Kc	0.8209			0.8140			0.8278			0.8347		

Table 6.4 Accuracy assessment of LULC classification results using SVM

Year	2000			2005			2009			2014		
LULC class	PA (%)	UA (%)	F-score (%)	PA (%)	UA (%)	F-score (%)	PA (%)	UA (%)	F-score (%)	PA (%)	UA (%)	F-score (%)
Agricultural Land	83.33	87.63	85.43	83.50	88.66	86.00	86.27	88.89	87.56	86.27	89.80	88.00
Dense vegetation	84.27	92.59	88.24	82.02	92.41	86.90	85.39	93.83	89.41	85.39	92.68	88.89
Sparse vegetation	84.91	86.54	85.71	86.79	88.46	87.62	89.62	87.96	88.79	86.79	87.62	87.20
Fallow land	89.47	77.98	83.33	91.58	80.56	85.71	91.58	81.31	86.14	91.58	83.65	87.44
Built up	88.79	90.48	89.62	88.79	91.35	90.05	88.79	94.06	91.35	90.65	94.17	92.38
Water bodies	86.02	97.56	91.43	87.10	97.59	92.05	87.10	98.78	92.57	92.47	98.85	95.56
Sand	89.53	77.00	82.80	93.02	76.92	84.21	93.02	80.00	86.02	93.02	80.81	86.49
OA (%)	86.58			87.48			88.79			89.38		
Kc	0.8433			0.8553			0.8691			0.8760		

6.4.3 LULC distribution

The area distribution of LULC classes for four different years 2000, 2005, 2009 and 2014 using different classification algorithms are shown in Table 6.5. On the other hand, it is significant to note that each of the three adopted image classification techniques gave a different area estimate. It is obvious as the selection of classification techniques has an impact on the area estimate. Since, SVM classification method was found to be the best by analyzing the Kc and OA results. Therefore, only the area estimates provided by SVM method were taken into consideration for the LULCC analysis. The classified LULC maps produced by implementing the SVM for different years are shown in Figure 6.4 (a, b, c, d). The proportion of total area covered by created LULC classes on the remote sensing images provides an insight of the composition of study area and shown in Figure 6.5. The present study indicates that in the year 2000, the agricultural land covered 1078 km^2 (70.34%) of the total area followed by dense vegetation 157.14 km^2 (10.25%), sparse vegetation 139.13 km^2 (9.08%), fallow land 76.29 km^2 (4.98%), built up 42.75 km^2 (2.79%), water bodies 25.33 km^2 (1.65%) and sand 14.05 km^2 (0.92%). In the year 2005, the agricultural land covered 856.89 km^2 (55.90%) of the total area followed by dense vegetation 21.73 km^2 (1.42%), sparse vegetation 342.31 km^2 (22.33%), fallow land 221.43 km^2 (14.45%), built up 55.74 km^2 (3.64%), water bodies 22.66 km^2 (1.48%) and sand 12.15 km^2 (0.79%). In the year 2009, the agricultural land covered 967.85km^2 (63.14%) of the total area followed by dense vegetation 17.98 km^2 (1.17%), sparse vegetation 226.82 km^2 (14.80%), fallow land 217.86 km^2 (14.21%), built up 67.64 km^2 (4.41%), water bodies 19.81 km^2 (1.29%) and sand 14.95 km^2 (0.98%). While in the year 2014, the agricultural land covered 907.76 km^2 (59.22%) of the total area followed by dense vegetation 72.15 km^2 (4.71%), sparse vegetation 329.30 km^2 (21.48%), fallow land 33.57 km^2 (2.19%), built up 121.67 km^2 (7.94%), water bodies 28.70 km^2 (1.87%) and sand 39.76 km^2 (2.59%). The year wise distribution of built up class are represented in Figure 6.6.

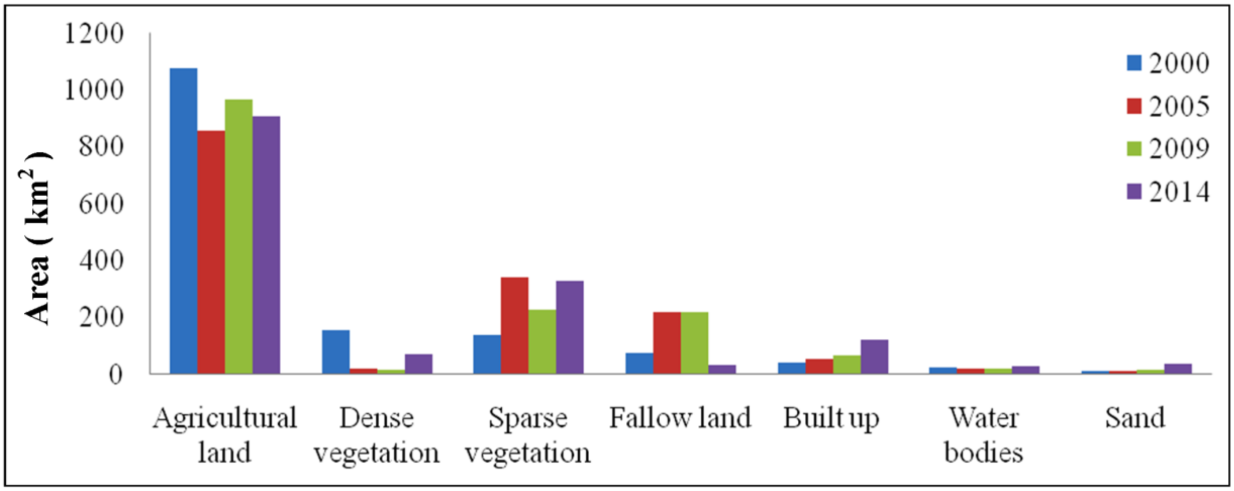

Figure 6.5 The distribution of LULC classes in different years

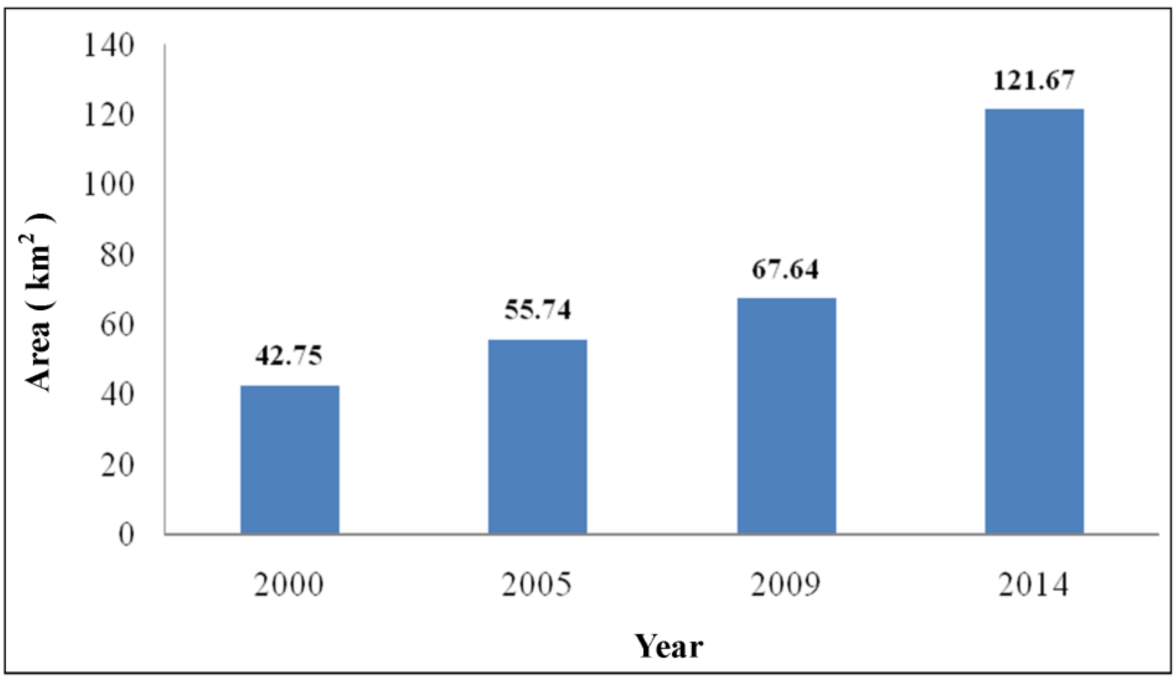

Figure 6.6 The distribution of built up class in different years

Table 6.5 LULC distribution for years 2000, 2005, 2006, and 2014 using MLC, ANN, and SVM algorithms (*Percentage area is given in brackets)

Year	2000 Area (km^2)*			2005 Area (km^2)*			2009 Area (km^2)*			2014 Area (km^2)*		
LULC classes	MLC	ANN	SVM	MLC	ANN	SVM	MLC	ANN	SVM	MLC	ANN	SVM
AL	1104.24 (72.04)	1075.03 (70.13)	1078.23 (70.34)	1141.45 (74.46)	848.26 (55.34)	856.89 (55.90)	1102.62 (71.93)	996.69 (65.02)	967.85 (63.14)	1051.78 (68.61)	878.36 (57.30)	907.76 (59.22)
DV	94.75 (6.18)	156.07 (10.18)	157.14 (10.25)	43.93 (2.87)	21.49 (1.40)	21.73 (1.42)	18.46 (1.20)	15.62 (1.02)	17.98 (1.17)	34.87 (2.27)	85.56 (5.58)	72.15 (4.71)
SV	226.68 (14.79)	161.51 (10.54)	139.13 (9.08)	72.81 (4.75)	364.52 (23.78)	342.31 (22.33)	242.29 (15.81)	203.72 (13.29)	226.82 (14.80)	232.72 (15.18)	322.89 (21.06)	329.30 (21.48)
FL	47.32 (3.09)	66.74 (4.35)	76.29 (4.98)	177.82 (11.60)	214.30 (13.98)	221.43 (14.45)	85.57 (5.58)	223.63 (14.59)	217.86 (14.21)	56.59 (3.69)	62.41 (4.07)	33.57 (2.19)
BU	28.62 (1.87)	33.95 (2.21)	42.75 (2.79)	48.96 (3.19)	51.19 (3.34)	55.74 (3.64)	53.39 (3.48)	57.52 (3.75)	67.64 (4.41)	101.88 (6.65)	115.20 (7.51)	121.67 (7.94)
WB	19.52 (1.27)	26.06 (1.70)	25.33 (1.65)	27.57 (1.80)	22.33 (1.46)	22.66 (1.48)	17.60 (1.15)	21.25 (1.39)	19.81 (1.29)	22.49 (1.47)	26.56 (1.73)	28.70 (1.87)
SA	11.78 (0.77)	13.55 (0.88)	14.05 (0.92)	20.36 (1.33)	10.82 (0.71)	12.15 (0.79)	12.98 (0.85)	14.48 (0.94)	14.95 (0.98)	32.58 (2.13)	41.93 (2.74)	39.76 (2.59)
Total	1532.91			1532.91			1532.91			1532.91		

6.4.4 Assessment of LULCC

The changes occurred in various LULC classes were assessed during period 1, period 2, period 3 and period 4 by adopting post-classification technique based on SVM based classified maps. The amount of LULCC during period 1, period 2, period 3 and period 4 are presented in Tables 6.6, 6.7, 6.8 and 6.9 respectively.

Table 6.6 Amount of LULCC during period 1 (2000-2005)

Year	2000		2005		Change 2000-2005		
LULC class	Area (km^2)	Area (%)	Area (km^2)	Area (%)	Changed area (km^2)	Changed area (%)	Annual rate of change
Agricultural land	1078.23	70.34	856.89	55.90	-221.33	-14.44	-4.60
Dense vegetation	157.14	10.25	21.73	1.42	-135.41	-8.83	-39.57
Sparse vegetation	139.13	9.08	342.31	22.33	203.18	13.25	18.01
Fallow land	76.29	4.98	221.43	14.45	145.14	09.47	21.31
Built up	42.75	2.79	55.74	3.64	12.99	0.85	5.31
Water bodies	25.33	1.65	22.66	1.48	-2.67	-0.17	-2.23
Sand	14.05	0.92	12.15	0.79	-1.90	-0.13	-2.91

Table 6.7 Amount of LULCC during period 2 (2005-2009)

Year	2005		2009		Change 2005-2009		
LULC class	Area (km^2)	Area (%)	Area (km^2)	Area (%)	Changed area (km^2)	Changed area (%)	Annual rate of change
Agricultural land	856.89	55.90	967.85	63.14	110.96	7.24	3.04
Dense vegetation	21.73	1.42	17.98	1.17	-3.75	-0.25	-4.73
Sparse vegetation	342.31	22.33	226.82	14.80	-115.50	-7.53	-10.29
Fallow land	221.43	14.45	217.86	14.21	-3.57	-0.24	-0.41
Built up	55.74	3.64	67.64	4.41	11.90	0.77	4.84
Water bodies	22.66	1.48	19.81	1.29	-2.85	-0.19	-3.36
Sand	12.15	0.79	14.95	0.98	2.80	0.19	5.18

Table 6.8 Amount of LULCC during period 3 (2009-2014)

Year	2009		2014		Change 2009-2014		
LULC class	Area (km^2)	Area (%)	Area (km^2)	Area (%)	Changed area (km^2)	Changed area (%)	Annual rate of change
Agricultural land	967.85	63.14	907.76	59.22	-60.09	-3.92	-1.28
Dense vegetation	17.98	1.17	72.15	4.71	54.17	3.54	27.79
Sparse vegetation	226.82	14.80	329.30	21.48	102.48	6.68	7.46
Fallow land	217.86	14.21	33.57	2.19	-184.29	-12.02	-37.40
Built up	67.64	4.41	121.67	7.94	54.03	3.53	11.74
Water bodies	19.81	1.29	28.70	1.87	8.89	0.58	7.41
Sand	14.95	0.98	39.76	2.59	24.81	1.61	19.56

Table 6.9 Amount of LULCC during period 4 (2000-2014)

Year	2000		2014		Change 2000-2014		
LULC class	Area (km^2)	Area (%)	Area (km^2)	Area (%)	Changed area (km^2)	Changed area (%)	Annual rate of change
Agricultural land	1078.23	70.34	907.76	59.22	-170.46	-11.12	-1.23
Dense vegetation	157.14	10.25	72.15	4.71	-84.99	-5.54	-5.56
Sparse vegetation	139.13	9.08	329.30	21.48	190.17	12.40	6.15
Fallow land	76.29	4.98	33.57	2.19	-42.71	-2.79	-5.86
Built up	42.75	2.79	121.67	7.94	78.93	5.15	7.47
Water bodies	25.33	1.65	28.70	1.87	3.37	0.22	0.89
Sand	14.05	0.92	39.76	2.59	25.71	1.67	7.43

During the period 1, the area occupied by agricultural land was reduced from 1078.23 km^2 to 856.89 km^2. However, it was increased to 967.85 km^2 during period 2. Later, it is again found to decrease from 967.85 km^2 to 907.76 km^2 during the period 3. While, during the entire period 4 of our study, the area covered by agricultural land under investigation was decreased from 1078.23 km^2 to 907.76 km^2. During the periods 1, 2 and 4, the areas occupied by the dense vegetation were found to decrease from 157.14 km^2 to 21.73 km^2, 21.73 km^2 to 17.98 km^2 and 157.14 km^2 to 72.15 km^2 respectively while during period 3; it was increased from 17.98 km^2 to 72.15 km^2. During the periods 1, 3 and 4 the areas covered by sparse vegetation were found to increase from 139.13 km^2 to 342.31 km^2, 226.82 km^2 to 329.30 km^2 and 139.13 km^2 to 329.30 km^2 respectively while during period 2, it was decreased from 342.31 km^2 to 226.82 km^2. During the period 1, the area occupied by fallow land was increased from 76.29 km^2 to 221.43 km^2, while during periods 2, 3 and 4, it was decreased from 221.43 km^2 to 217.86 km^2, 217.86 km^2 to 33.57 km^2 and 76.29 km^2 to 33.57 km^2 respectively. On the other hand, during the periods 1, 2, 3 and 4, the area occupied by built up was regularly increased from 38.75 km^2 to 55.74 km^2, 55.74 km^2 to 67.64 km^2, 67.64 km^2 to 121.67 km^2 and 38.75 km^2 to 121.67 km^2 respectively. During the periods 1 and 2, the area occupied by water bodies was decreased from 25.33 km^2 to 22.66 km^2 and 22.66 km^2 to 19.81 km^2. While during periods 3 and 4, it was increased from 19.81 km^2 to 28.70 km^2 and 25.33 km^2 to 28.70 km^2. During the period 1, the area occupied by sand was decreased from 14.05 km^2 to 12.15 km^2. While during periods 2, 3 and 4, it was increased from 12.15 km^2 to 14.95 km^2, 14.39 km^2 to 39.76 km^2 and 14.05 km^2 to 39.76 km^2 respectively. Since, the results of spectral separability analyses showed comparatively low separability values between agricultural land and sparse vegetation (Table 6.1). It may be one of the reasons of increase in sparse vegetation during periods 1, 2 and 3 due to its misclassification at some places with agricultural land and dense vegetation classes. The agricultural land covered an area of 1078.23 km^2 in 2000 (70.34% of total area) and it was gradually found to be decrease to 856.89 km^2 (55.90%), 967.85 km^2 (63.14%) and 907.76% (59.22%) in years 2005, 2009 and 2014 respectively. In year 2000, it is observed that the built up covered an area of 42.75 km^2 (2.79%) and it progressively increased to 55.74 km^2 (3.64%), 67.64 km^2 (4.41%) and 121.67 km^2 (7.94%) in 2005, 2009 and 2014 respectively. A diagrammatic representation of LULCC during period 1, period 2, period 3 and period 4 in Varanasi district are shown in Figure 6.7.

During 2000-2014, the rate of loss of agricultural land was found maximum with -1.23% followed by fallow land with -5.86% and dense vegetation with -5.56%. While, the built up showed highest positive rate of change with 7.47% followed by sand with 7.43%, sparse vegetation with 6.15% and water bodies with 0.89%. It clearly indicated that, built up had highest positive rate of change while, agricultural land had highest negative rate of change. The major cause for this type of trend is the rapid conversion of agricultural land and fallow land into built up due to population growth and need for residential land. The detailed information about the rate of change for individual LULC class during period 1, period 2, period 3 and period 4 are shown in Tables (6.6-6.9).

The change values for LULC classes during all the periods estimated through SVM are shown in Figure 6.8. The areas that converted from one LULC class into other during 2000-2014 are shown in Figure 6.9 (a). While, only the areas that changed from agricultural land into built up over a given time period are shown in Figure 6.9 (b).

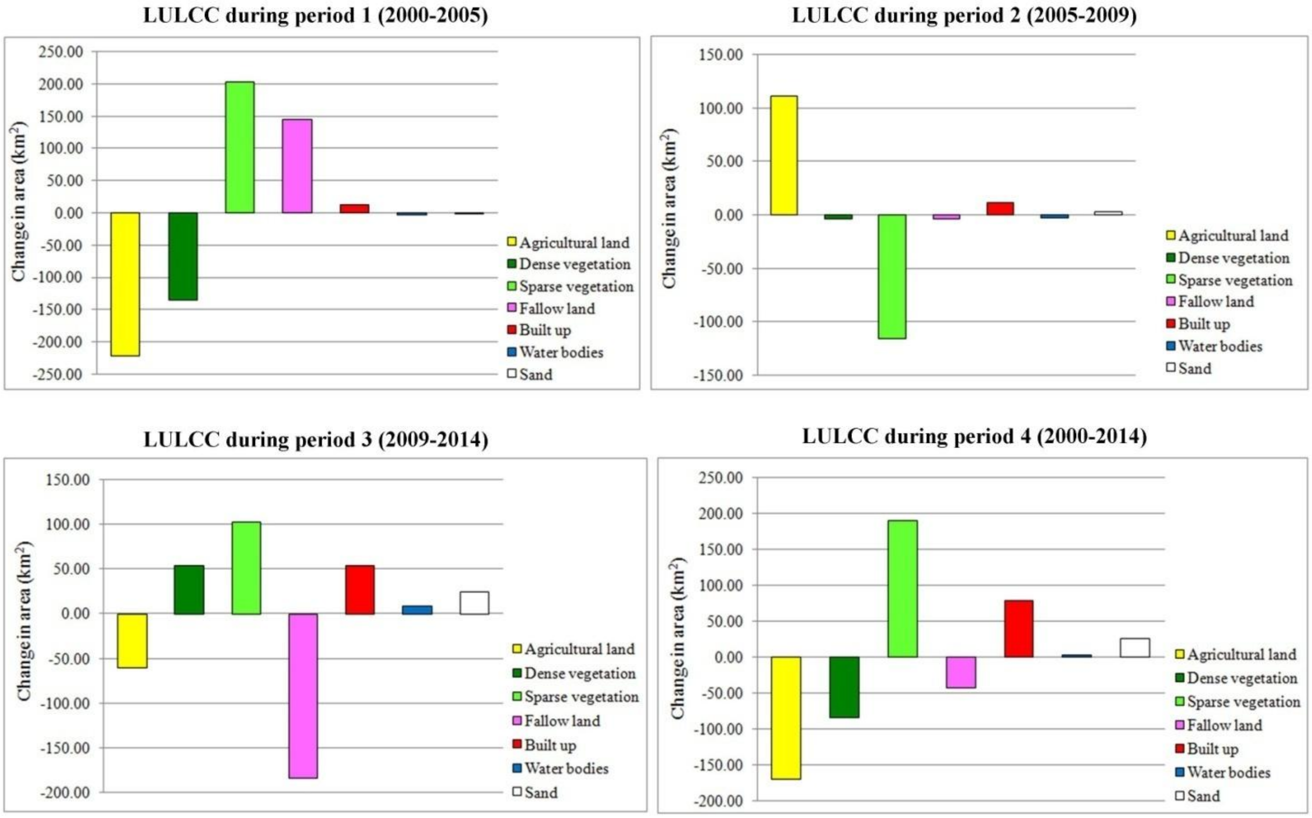

Figure 6.7 Diagrammatic illustration of LULCC (in km^2) during the period 1, period 2, period 3, and period 4

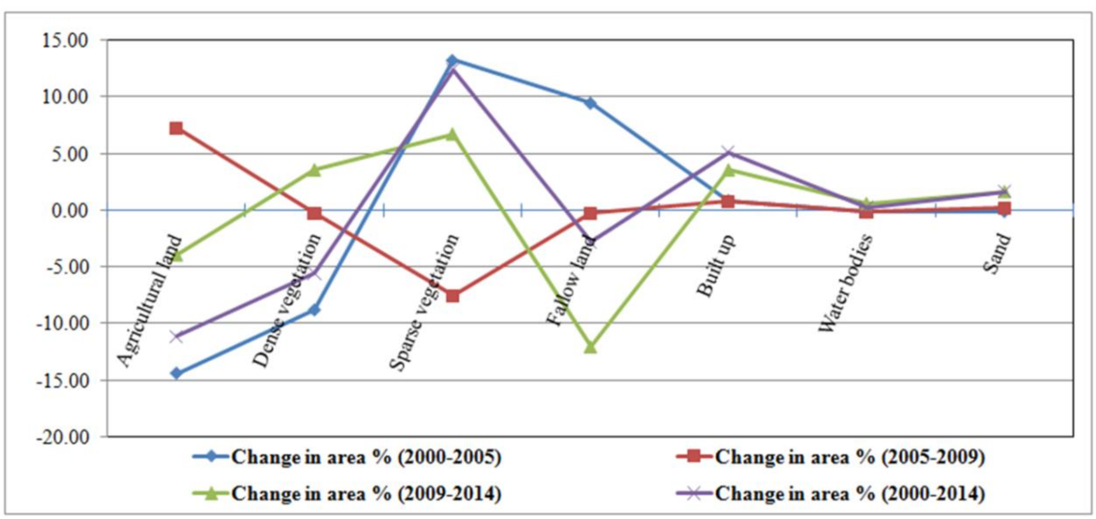

Figure 6.8 The change values for LULC classes (in %) estimated through SVM during the period 1, period 2, period 3, and period 4

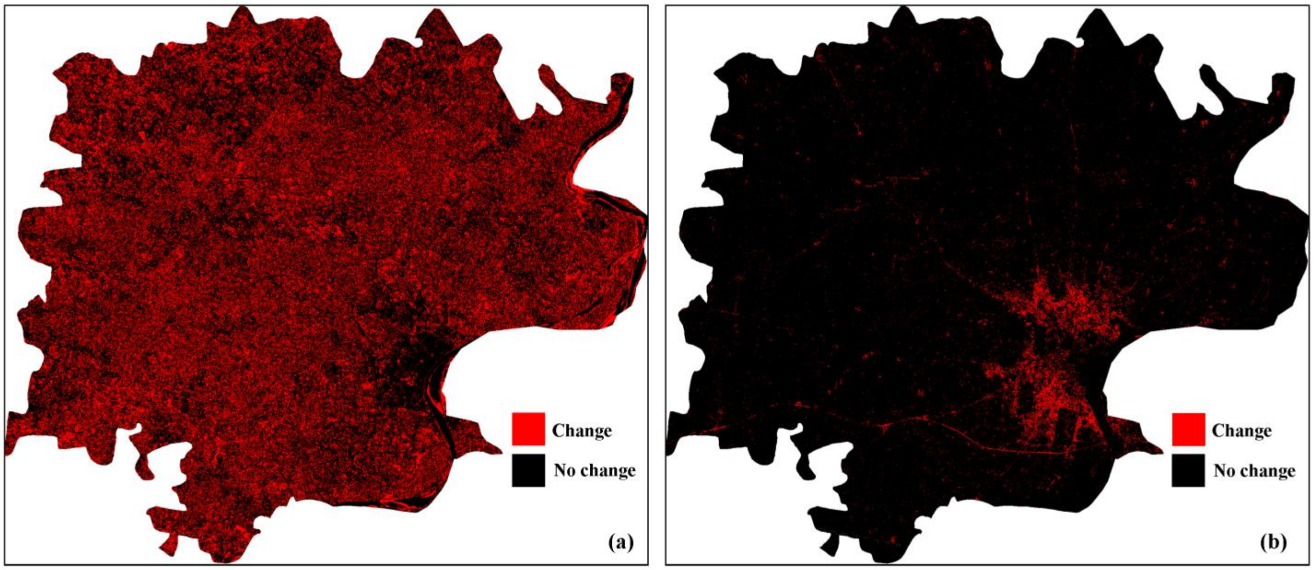

Figure 6.9 (a) The areas that converted from one LULC class into other, (b) Only the areas that changed from agricultural land into built up during the period 2000-2014

The statistical analyses using paired samples t-test were carried out on data produced from the classified remote sensing images of the study area and are shown in Tables 6.10, 6.11 and 6.12. The paired samples t-test is applied to compare the mean values of two study periods, and calculate the difference between the two periods, then test to observe if the average difference is considerably different from zero. Table 6.10 indicates that the year 2005 reports the least values in terms of mean, standard deviation (SD) and standard error of mean (SEM) whereas, the year 2000 reveals the highest values for all descriptive statistical parameters. The test correlation results are shown in Table 6.11. The strongest correlation is found to be in pair 2 between the years 2005 and 2009. Also, the significance value of pair 2 illustrates that there is a significant difference between the means of the two study years (2005 and 2009). The results of the paired sample t-test (Table 6.12) demonstrate that the *p*-values (sig. (2-tailed)) for all the paired categories are greater than 0.05. Therefore, it reveals that there are no statistically significant differences in the overall LULCC between all four pairs of study periods evaluated. Although, it does not essentially signifies the absence of overall changes in LULC over the analyzed study periods. The test merely states that the observed changes do not correspond to a significant quantity in statistical terms. In other words, the aggregated changes in LULC between the study periods are insignificant, even though there are changes exist within individual LULC classes that can be regarded to be significant.

Table 6.10 Statistics of paired samples

Pairs		Mean	N	SD	SEM
Pair1	Year 2000	218.986	7	382.844	144.701
	Year 2005	218.987	7	307.957	116.397
Pair2	Year 2005	218.987	7	307.957	116.397
	Year 2009	218.986	7	342.897	129.602
Pair3	Year 2009	218.986	7	342.897	129.602
	Year 2014	218.987	7	321.538	121.529
Pair 4	Year 2000	218.986	7	382.844	144.701
	Year 2014	218.987	7	321.538	121.529

Table 6.11 Correlation between paired samples

Paired Categories		N	Correlation	Sig.
Pair 1	Year 2000 & Year 2005	7	0.9320	0.00223
Pair 2	Year 2005 & Year 2009	7	0.9853	4.91478 E-5
Pair 3	Year 2009 & Year 2014	7	0.9607	5.72704 E-4
Pair 4	Year 2000 & Year 2014	7	0.9603	5.89747 E-4

Table 6.12 Paired samples t-test

Paired Categories		95% confidence interval of the differences		T	df	Sig. (2-tailed)
		Lower	Upper			
Pair 1	Year 2000 - Year 2005	-136.05643	136.05497	-1.31031E-5	6	0.9999
Pair 2	Year 2005 - Year 2009	-60.68684	60.68752	1.3824E-5	6	0.9999
Pair 3	Year 2009 - Year 2014	-88.24272	88.24214	-7.92267E-5	6	0.9999
Pair 4	Year 2000 - Year 2014	-107.57034	107.56899	-1.52731E-5	6	0.9999

6.5 CONCLUSION

In the present work, the SVM was found to provide more reliable and realistic results for classification of remote sensing images in comparison to ANN and MLC at the observed scale for study area. The SVM provided the best classification results with OA of 86.58%, 87.48%, 88.79% and 89.38% for the images of years 2000, 2005, 2009 and 2014, respectively. It is not possible for SVM to outperform ANN in all situations, but so far, there are no comprehensible recommendations on their selections in practical projects. Therefore, it is needed to explore more experimental and theoretical studies to decide under what conditions SVM is better than the others. Furthermore, the characteristics of study area such as number of LULC classes, the selection and size of training samples, the pre-processing steps for the corresponding datasets dates play a considerable role in the quality and effectiveness of the final classification images. Therefore, all these parameters should be taken into consideration in order to achieve reasonable classification results.

The outcomes of this study revealed that, during 2000-2014, the area covered by agricultural land was decreased by 170.46 km^2. The area covered by dense vegetation was decreased by 84.99 km^2. The area covered by sparse vegetation was increased by 190.17

km^2. The area covered by fallow land was decreased by 42.71 km^2. The built up land was increased by 78.93 km^2. The area cover by water bodies was increased by 3.37 km^2. The sand area was increased by 25.71 km^2. The results achieved clearly illustrate the extensive changes in LULC in Varanasi district. It can be perceived easily that the increased quantity of built up area over the specified time period results in decrease of area covered by agricultural land and dense vegetation etc. The t-test reveals that the observed changes do not correspond to a significant quantity in statistical terms. In other way, the collective changes in LULC between the study periods are insignificant.

This study also illustrates the effectiveness of multi-temporal Landsat images for the analysis and quantification of LULCC in an area. However, the LULC classification accuracy and change analysis are strongly affected by the moderate spatial resolution of the Landsat images. So, in future, the high resolution remote sensing images and longer time period should be used to get improved change analysis results of such highly heterogeneous area. In addition, the causes affecting the LULCC in conjunction with socio-economic factors and environmental variables could also be observed.